energy&fuels
Article
Cite This: Energy Fuels 2019, 33, 6904−6920
pubs.acs.org/EF

Surfactant-Assisted Spontaneous Imbibition to Improve Oil Recovery on the Eagle Ford and Wolfcamp Shale Oil Reservoir: Laboratory to Field Analysis

I Wayan Rakananda Saputra,* Kang Han Park, Fan Zhang, Imad A. Adel, and David S. Schechter

Harold Vance Department of Petroleum Engineering, Texas A&M University, College Station, Texas 77843, United States

ABSTRACT: Abundant resources being left behind at the end of the short production life of an unconventional liquid-rich reservoir (ULR) well has inspired many to investigate methods to improve the recovery. One eminent method is through the addition of surfactant during the completion stage of the well. Through numerous published laboratory studies, it can be concluded that this process possesses a promising potential in improving overall well productivity. Several field-scale results gathered from public data sources also confirmed the laboratory-scale study by correlating the effect of surfactants to the improvement of the estimated ultimate recovery (EUR). However, the absence of independency on those field-scale results often casts doubt on the actual efficacy of the method. The lack of field-scale information in the realm of scientific publications contributes to the limited understanding of surfactant application. This study is to fulfill the obvious need of field-scale studies on the application of surfactant by surfactant-assisted spontaneous imbibition (SASI) during completion of wells in the ULR. Numerical-based upscaling through modification of capillary pressure and relative permeability of the laboratory-scale experimental results provides a view on the effectiveness of this method on the field scale. Comparison is performed between the initial oil production rate, cumulative oil, and cumulative water production. A complete set of the laboratory-scale experimental studies is also included and consists of interfacial tension, contact angle, zeta potential, adsorption isotherm, and CT-assisted spontaneous imbibition. CT-scan technology is incorporated as well in the construction of a core-scale numerical grid model to model the heterogeneity of the shale core plug sample. In the end, sensitivity analysis is also executed to analyze the effect of different reservoir properties and SASI-related completion parameters on the efficiency of the method. There are four main takeaways of this comprehensive study. First, a complete and robust workflow on investigating SASI performance is compiled and tested. This workflow consists of a laboratory-scale experimental study as well as a numerical-based field-scale investigation and can be applied to different shale reservoirs as well as different surfactants. Second, three different surfactants are tested in this study with significant well production improvement observed, thus confirming the increment of production observed in the laboratory-scale study. These results are also compared to other lab-scale experiments conducted with different ULR samples to verify and strengthen the effectiveness of SASI. Third, sensitivity analysis shows that SASI improves well productivity for a variety of fracture and matrix properties. We observed a range of matrix and fracture properties where SASI performs optimally, and last, an independent field data study is provided. This actual case study is done carefully to isolate the effect of SASI on the well production. An agreement on the range of production improvement by SASI between the field data analysis and the numerical field-scale model is also observed.

■ INTRODUCTION

It is ironic when the highly abundant resource of shale oil comes in tandem with extremely low recovery factors, not to mention the fast decline rate of 14% as well as the average well economical lifetime of a mere 36 months.[1] On the bright side, the circumstances allow for a vast research area for ULR recovery improvement to develop. Numerous enhanced oil recovery (EOR) methods have been explored with the mechanism narrowing down to wettability alteration using surfactant or salt and through the utilization of gas. The primary production mechanism in shale is still currently a hot topic with a general consensus on how hydrocarbon is being produced has not been achieved. With that in mind, exploring the three enhanced recovery mechanisms listed above has proven to be even more intriguing, if not challenging. Several publications have shown proof that the three mechanisms do increase oil production.[2−8] In addition, more interesting observations, such as color shift in the produced oil,[9] unique production profile,[10] and the independency of recovery from minimum miscibility pressure (MMP),[2] keep the idea interesting and reiterate the opinion that shale is a completely different rock, and we are still barely scratching the surface in understanding the production from shale.

Surfactant application on the shale reservoir has been extensively studied in the laboratory-scale experiments. Spontaneous imbibition experiments are usually chosen as the concluding test to assess the efficacy of surfactant on improving the production of oil from a shale core plug. The experiment is accompanied by initial testing of surfactant in an oil−water−rock system through emulsion stability, interfacial tension (IFT), zeta potential (ZP), contact angle (CA), and adsorption. It is proven that surfactant improves oil production as shown by multiple publications of work done on the three most prominent shale oil plays in the US, Wolfcamp, Eagle

Received: January 22, 2019
Revised: June 18, 2019
Published: July 31, 2019

DOI: 10.1021/acs.energyfuels.9b00183
Energy Fuels 2019, 33, 6904−6920

Ford, and Bakken. On the Wolfcamp shale oil play, four different surfactant types were tested by Alvarez and Schechter on the two available Wolfcamp lithologies with their results confirming production enhancement when surfactant is added into the system. It was found that anionic surfactant works the best on quartz-rich rock, while on carbonate-rich Wolfcamp, the cationic surfactant performed dominantly.[11] Production improvement by the addition of surfactant was also observed on the Bakken[3,12−14] and Eagle Ford[15−18] systems.

The successful laboratory study of surfactant application on the shale oil rock sample leads to the increasing interest in the mechanism of the method, which is highly important to understand when field-scale implementation is the final objective. Surfactants have been extensively studied for conventional EOR; however, the application of low concentration surfactants during completion in unconventional liquid-rich reservoir (ULR) is not as common. There are three forces that are known to cause fluid movement in the pore system of the rock: viscous, gravity, and capillary. The ultralow permeability characteristic of the shale rock sample as well as the experimental condition of this method make the first two generally negligible, leaving capillary pressure as the dominant cause of fluid movement. As shown by the definition of capillary pressure by Young and Laplace, surface wettability and interfacial tension (IFT) have a strong impact on the capillary pressure. Wettability of the surface determines the direction of the pressure. Oil-wet wettability state will result in the direction of the capillary pressure which causes the oil to be trapped inside the pore, while the water-wet state causes the expulsion of oil. On the other hand, the magnitude of IFT only controls the magnitude of capillary pressure, not the direction of the pressure. The surfactant molecule alters both interfacial tension of oil and water as well as the wettability of the rock surface. Specifically, it reduces the IFT and alters the wettability from oil-wet to water-wet. Therefore, it can be summarized that surfactant enhances recovery by improving the performance of the capillary-driven spontaneous imbibition through alteration of IFT and wettability. Surfactant-assisted spontaneous imbibition (SASI) will be used frequently in this work to refer to the method.

Wettability alteration is found to be an important aspect of the application of SASI on most of the shale oil reservoirs in the US due to their strongly oil-wetting original wettability.[19] Therefore, wettability alteration from the oil-wet to the water-wet region is critical for SASI to be successful. Surfactant alters the wettability through the adsorption mechanism as its hydrophobic tail attaches to the oil-wet surface of the rock, causing its hydrophilic head to face the pore space as a water-wet layer. Wettability alteration through adsorption was investigated comprehensively by comparing surfactant adsorption, wettability, and zeta potential with the result showing a positive correlation between the three measured properties, indicating that the adsorption-based alteration mechanism does occur on the rock surface.[20] Atomic Force Microscopy provides physical evidence of this mechanism by comparing the image of the rock surface before and after interaction with the surfactant.[21−23] In the same study, it can also be observed that oil-wet is caused by adsorption of the heavier end of the hydrocarbon chain on the rock surface.

Numerical modeling of the capillary-driven imbibition process is achieved by adding the capillary pressure curve on the model.[24−26] In the previous discussion, it was concluded that surfactant enhances the capillary-driven spontaneous imbibition by improving the capillary pressure to expulse more oil out of the pore. Therefore, numerical modeling of SASI should be done by the addition of capillary pressure curve modification function as based on the amount of surfactant contained in each grid. There are numerous studies published on how to model the involvement of surfactant in a capillary-driven spontaneous imbibition process. Adibhatia et al. presented the application of a surfactant concentration−IFT relation coupled with IFT−trapping number correlation to model the change in capillary pressure and relative permeability function.[27] Similar surfactant concentration to IFT correlation was used by Delshad et al.; however, capillary desaturation curves were used instead of trapping number to include the alteration in the flow properties.[28] An additional method to include the surfactant-induced alteration of capillary pressure and relative permeability was presented through the application of a time function.[29,30] However, the unique characteristic of a shale oil reservoir requires a new method to numerically model the process of SASI on a shale oil system due to the unavailability of both time-dependent function and trapping number in an unconventional liquid reservoir.[31]

This study aims to provide a method to investigate the field-scale impact of SASI on the Eagle Ford reservoir, based on numerical-based upscaling of laboratory-scale experimental results. The measurement of multiple surfactant-related properties is also included in this study, including the spontaneous imbibition experiment. In addition, supplementary experimental data are provided as well to verify the ability of surfactant to improve oil recovery from the Permian basin. Then, a laboratory-scale numerical model based on the laboratory experiment is constructed to gather the capillary pressure and relative permeability curves for upscaling purposes. The field-scale impact of SASI then can finally be calculated by applying both curves on a field-scale model. In addition to the ability to give a view on the field-scale effect of SASI, this study gives a comprehensive procedure to assess different surfactants on their ability to improve production through SASI, starting from the laboratory experiment to the field-scale result that can be applied on any surfactant and any ULR formation. To better understand the impact of different reservoir properties on the performance of SASI, a sensitivity analysis study is also included in this work. A novel real field case study comparing the base case of the well without surfactant addition and the surfactant-treated well on the Wolfcamp formation is also presented to complete the field-scale study. This study however is not aimed to answer the ongoing debate on the optimization of surfactant quantity to be added into the completion fluid. Optimization of the actual field-scale application of SASI directly implies the need for economic analysis of the method. Since economics is not part of the scope, concentration optimization is not included in the objective of this work.

■ METHODOLOGY

The ultimate objective of this study is to provide an assessment on the field-scale impact of SASI, in order to improve the depth of the common laboratory-scale study on surfactant application on the shale oil reservoir. In order to achieve this objective, the numerical modeling method is utilized to upscale the laboratory-scale result for a field-scale analysis. The main concept of the upscaling work is implementing the surfactant-induced capillary pressure and relative permeability modification on a generic field-scale model. Capillary pressure and relative permeabilities are constructed by history-matching oil production from spontaneous imbibition experiments

DOI: 10.1021/acs.energyfuels.9b00183
Energy Fuels 2019, 33, 6904−6920

through numerical modeling of the experiment, done on a CT-based core plug model. The addition of the upscaling section to the laboratory-scale study will complete the workflow of assessing surfactant efficacy for SASI application.

To demonstrate the utilization of the workflow, an entirely new laboratory work is performed instead of citing a previously done laboratory-scale study. This comprehensive workflow is divided into three big parts. First is the laboratory experimental works where all data on the interaction of surfactant to the oil−water−rock system are gathered. Second, a laboratory-scale numerical simulation is done to construct the required properties for the upscaling process. Lastly, the field-scale numerical work, where the field-scale impacts of SASI are studied, as well as numerous sensitivity analyses of the production enhancement on reservoir and surfactant-related properties are studied.

Laboratory Experiments. Several experimental procedures are included in the laboratory experiments part of this study. Properties of rock, oil, and surfactant used are gathered first, followed by sample preparation for the experimental procedure. Interfacial tension (IFT), zeta potential (ZP), contact angle (CA), surfactant adsorption, and spontaneous imbibition experiments are then conducted. These sets of experiments are designed to give a sufficient understanding of the capillary-driven spontaneous imbibition process, as each measurement studies the interaction of surfactant with different phases. Ultimately, the result of the spontaneous imbibition experiment will serve as the basis for the upscaling process.

Rock, Oil, and Surfactant Properties and Sample Preparation. To ensure the representability and the accuracy of this study, field-retrieved rock and oil samples are used for all of the laboratory procedures done. One inch diameter with two inch length sidewall core plugs are used for the spontaneous imbibition, and several rock trims are also gathered for contact angle, zeta potential, and adsorption measurement. Results from the XRD analysis show that the Eagle Ford rock sample is carbonate-rich with calcite minerals composing more than 50% of the rock. Some amounts of clays and quartz mineral are also found in the rock sample. Standard petrophysical analysis of the rock is also given by the provider of the core sample with the porosity value of 8.7% and 200 nd air permeability.

Initial saturation and wettability of the rock samples are restored by implementing cleaning and aging procedures. Rock samples are cleaned through the Dean−Stark apparatus in toluene and methanol sequentially, which is then followed by vacuum drying. After the cleaning process, rock samples are submerged or aged in their corresponding oil sample under reservoir temperature and ambient pressure. This aging process for core plugs which will be used on the imbibition experiments runs for at least four months, while smaller rock chips for contact angle measurement are aged for at least 2 weeks. Original-oil-in-place (OOIP) for recovery factor calculations on the spontaneous imbibition experiments are determined by measuring the change in weight before and after the aging process. More details on the aging process can be found in ref 19.

Along with sidewall core plugs, oil sample is also retrieved from another well in the area, to ensure the representability of the reservoir condition in the laboratory experiment. The working temperature for the Eagle Ford is selected to be 180 °F, lower than the actual reservoir temperature where rock and oil samples are retrieved. The selection is done due to experimental restriction as the actual reservoir temperature of 220 °F is higher than the boiling temperature of water, which is used as the base fluid for the aqueous phase. Density is measured on the working temperature of the laboratory procedures, resulting in the density value of 0.7077 g/cc. In addition, total acid number (TAN) and total basic number (TBN) are also measured by automatic titration. TAN and TBN of the Eagle Ford oil are measured to be 0.1989 and 0.6100 mg-KOH/g-oil.

Four fluid systems are tested in this study with the Eagle Ford oil and rock system, consisting of three different surfactant solutions and one base case. Based on the composition as supplied by the MSDS, all three surfactants are anionic surfactants. Concentration is defined using a widely used field unit of gallon per thousand gallons or gpt where 1gpt corresponds to 0.1 vol % concentration. Table 1 describes the concentration and color coding of each fluid system which will be used consistently in this work. All surfactants in this study are commercially available, enabling a direct field application of the results observed in this study.

Table 1. Fluid System Concentration and Color Code for Eagle Ford Laboratory Data

Fluid System	Surfactant Concentration
DW	-
Surf1	2gpt
Surf2	1gpt
Surf3	1gpt

As mentioned previously, this study focuses on the application of the surfactant assessment workflow on the Eagle Ford. However, laboratory data of experiments done on the Permian sample are also added to demonstrate the universal application of SASI (Table 2).

Table 2. Fluid System Concentration and Color Code for Permian Laboratory Data

Fluid System	Surfactant Concentration
DW	-
SurfA	1gpt
SurfB	1gpt
SurfC	1gpt
SurfD	1gpt

XRD analysis concludes that the Permian rock sample is quartz-rich with 49% of quartz, 2% of calcite, and 22% of mica composing the sample. The porosity of the rock is determined to be 10% and 396 nd for the air permeability. The lower reservoir temperature of the Permian allows for the measurements to be done on the actual temperature of the reservoir, 155 °F. On this temperature, the oil density is measured to be 0.7700 g/cc. A different set of fluid systems are tested on the Permian sample consisting of one base case with no surfactants and four different surfactants with the concentration and color coding shown on the table below.

Interfacial Tension Measurement. Examination of IFT is highly essential in investigating SASI due to the IFT reduction effect of surfactant which, as shown by Young−Laplace's equation, leads to the alteration of capillary pressure. An inverted version of the pendant drop method is utilized in this study to measure the IFT between the aqueous phase and oleic phase. A J-shaped needle is used to dispense the oleic phase in a preheated aqueous phase in the upward direction. The evolution of the oil drop is recorded with a high-speed camera, and the exact moment when the drop detaches from the needle is captured and analyzed via a drop shape analyzer software. The density difference between the two phases on the respective temperature which is already measured beforehand is inserted to calculate the IFT value.

Zeta Potential Measurement. Surface charge and wettability can be analyzed from the zeta potential data of a rock particle. Surface charge, as well as the charge of the surfactant head, can be determined by the sign convention of the zeta potential, while comparing only the magnitude of zeta potential between the rock particles suspended in different aqueous phases gives an indication of the wetting state of the rock under each corresponding aqueous phase. In this study, zeta potential is measured with the Nanobrook ZetaPALS unit which utilizes laser-diffraction-based particle speed detection to determine the zeta potential of each sample tested. A pair of electrodes is submerged in the sample providing voltage difference which drives the rock particle suspended in the sample from one electrode to another. Zeta potential, then, is calculated in the built-in software by correlating the voltage applied to the speed of the rock particle.

Special sample preparation must be done for each of the zeta potential measurements. The rock sample from the sidewall cores is pulverized and filtered through the ASTM #325 sieve which filters out

DOI: 10.1021/acs.energyfuels.9b00183
Energy Fuels 2019, 33, 6904−6920

any particle larger than 45 μm. Pulverized rock is then mixed with the aqueous phase, which is filtered beforehand through a 0.2 μm syringe filter, for 1 min under a sonicator that is set on 40% amplitude. The suspension then is moved to a cuvette for the measurement.

Contact Angle Measurement. The wettability of a rock surface determines the direction of the capillary pressure as shown by the Young–Laplace equation. In this study, wettability is assessed by measuring the contact angle of an oil drop on a rock surface in the presence of the aqueous phase. By comparing the contact angle of the drop for the aqueous phase with or without surfactant, the degree of wettability alteration as caused by the surfactant molecule can be assessed. The captive bubble method is utilized for this measurement. A rock chip that has been previously prepared through the aging process is positioned on top of a stage which is submerged in the aqueous phase. The oil drop is dispensed on the tip of a J-shaped needle which then is used to position the oil drop on the bottom surface of the rock chip. The contact angle is calculated by processing the image of the oil drop in contact with the rock surface. Results are categorized into three different wettability conditions as based on the classification from Reed and Healy.[32] In order to use the classification, values from this measurement must be converted with the conversion shown in the equation below. Similar to the IFT measurement, the whole contact angle measurement is done under the working temperature of 180 °F.

$$CA = 180 - CA_m \tag{1}$$

Surfactant Adsorption Measurement. Surfactant molecules alter the wettability of the rock through adsorption, where its molecule attaches to the surface of the rock. On the numerical modeling section, surfactant adsorption is used to determine the extent to which the alteration of capillary pressure and relative permeabilities occurs. Having the information on the surfactant adsorption isotherm also gives information on the economical side of surfactant application as it controls the amount of surfactant needed in each treatment.

Measurement of surfactant adsorption in this work is done by indirect measurement. Change in the amount of surfactant before and after the solution is reacted with rock particles is observed and converted to an adsorption isotherm curve. UV spectroscopy is utilized to measure the surfactant concentration in the solution with calibration curve constructed beforehand. Work published by Alvarez et al. contains more details on the procedure of the measurement.[3] Adsorption measurement is done on various initial concentrations to construct the adsorption isotherm of each surfactant.

CT-Assisted Surfactant-Assisted Spontaneous Imbibition Experiments. Surfactant performance on improving oil production from SASI is evaluated by the imbibition experiments. This spontaneous imbibition experiment will provide an actual performance on how different fluid systems affect the oil production. The oil recovery curve from this experiment is used to investigate the improvement of both rate and quantity of recovery from different fluid systems. The same data will also be used to build the laboratory-scale model which then in the end will be upscaled to the field-scale dimension.

Four fluid systems are tested in this study using four different cleaned and aged core plugs. Each core plug is placed horizontally inside a modified Amott Cell which is filled with each corresponding fluid. Then, the Amott Cells are placed inside an oven to ensure the working temperature of 180 °F is achieved throughout the whole experiment, which typically runs for 10 days. The oil production data are constructed by periodically recording the produced oil volume on the graduated part of the Amott Cell.

In addition to the oil production data, the whole Amott Cell setup is also periodically scanned under the CT-Scan machine. Application of CT technology to the laboratory work of the petroleum industry brings one major advantage as it enables the visualization of fluid flow in the core plug without destroying the rock sample. A time-lapse illustration of fluid movement inside the core plug is formulated by periodic scanning. In this study, a Toshiba Aquilion TSX-101A CT-Scanner machine is utilized to gather all the CT-Scan data.

Laboratory-Scale Modeling. Following the laboratory experiments, a numerical model to model the spontaneous imbibition experiment is constructed. Enhancement of oil production through imbibition is driven by change in capillary action as surfactant interacts with the oil–water-rock system. Implementation of this concept to a numerical model is achieved by applying two kinds of capillary pressure curves which serve as a native and terminal capillary pressure curve. At time zero, all grid of the numerical model which represents the core plug has the native curve applied. As surfactant molecules move into each grid, a new curve is constructed by running a weighted-interpolation between the native and terminal curves. The amount of surfactant adsorbed, calculated from the measured surfactant adsorption isotherm, is used as the weighting factor. In addition to capillary pressure, relative permeability values are also affected by the addition of surfactant and is modeled through the same mechanism as the capillary pressure.

The final goal of this step is to construct the capillary pressure and relative permeability curves of each of the four tested fluid system. Obtained curves then will be applied on the field-scale modeling to upscale the laboratory data to the field-scale. Construction of the three curves are done by history-matching the oil production curve of the four spontaneous imbibition experiments. Initial curves are built based on the imbibition experiment done using the base case fluid system and final curves of each surfactant are created by history-matching each corresponding spontaneous imbibition experiment.

Shale rock samples is widely believed to be highly heterogeneous with multiple bedding planes, as well as microfractures, observed even in the core-scale dimension. Since the upscaling part of this work is solely based on the capillary pressure and relative permeability curves generated from history-matching the spontaneous imbibition laboratory experiments in this laboratory-scale modeling, it is consequential to build the core plug model as accurate as possible. Heterogeneity is modeled by building a porosity map of each plug in this study based on the CT-scan image. Each core plug is scanned after the cleaning process and before the aging process in order to remove any rock sample contaminants. Then by converting the CT-number to density and density to porosity, the porosity map is created. A permeability distribution map is also constructed, based on a porosity-permeability cross plot of Eagle Ford samples. In addition, grids are resized due to the large number of grids created from this process. Initial images from the CT machine could result in 50 million grid blocks for each core plug grid model. In this study, the grid number is brought down to 8000 grids to save running time. Then on this heterogeneous model, history-matching is done by manually configuring both curves to obtain the closest match to the oil production from the spontaneous imbibition experiment.

Field-Scale Modeling and Sensitivity Analysis. The final step of this study is the construction of the field-scale model which also includes sensitivity analysis of SASI performance to various reservoir properties. The modeling mechanism of SASI on the field-scale model is based on the modeling mechanism previously done on the laboratory-scale model. However, due to the difference in grid model type between the laboratory- and field-scale models, a number of modifications must be included. A single porosity model is utilized on the core plug grid model, while on the field-scale model, the model is executed in a dual porosity system. On the dual porosity field-scale model, initialization of the model is done by assuming the period after hydraulic fracturing to be time zero. Therefore, it can be safely assumed that at the initial condition the fracture network is saturated with the aqueous phase. Spontaneous imbibition then will occur as the aqueous phase from the fracture system is taken into the matrix in exchange of oil being expelled from the matrix into the fracture. A 10-day shut-in time is applied in the simulator to represent the period between well completion and well production.

The simulation is done on a synthetic model of a hydraulic fracture stage with 200 ft and 300 ft of stage spacing and half-length. All results from the model are multiplied by 20 to convert the result to well basis, assuming a 20-stage hydraulic fracture completion. Reservoir properties are gathered from multiple publications of Eagle Ford data to represent field data with the data attached in Table 3. Four models are run to compare the four fluid systems investigated in this

DOI: 10.1021/acs.energyfuels.9b00183
Energy Fuels 2019, 33, 6904–6920

study. Comparison is done by recording two oil production data, rate and cumulative recovery.

Table 3. Reservoir Properties of the Field-Scale Numerical Model

property	value	property	value
thickness (ft)	100	k_{HF} (md)	25
ϕ_m (frac.)	0.0867	fracture spacing (ft)	0.2
ϕ_f (frac.)	0.006	S_{wi} (frac.)	0.15
ϕ_{HF} (frac.)	0.2	P_i (psia)	9000
k_m (nd)	145	stage spacing (ft)	200
k_f (nd)	300	x_{HF} (ft)	300

In this study, sensitivity analysis on the field-scale model is done by analyzing the effect of multiple reservoir and completion properties on the performance of SASI. Reservoir properties analyzed include matrix porosity, matrix permeability, fracture porosity, fracture permeability, and fracture spacing, while completion parameters include shut-in time and surfactant concentration. Change of value on the properties listed before would also automatically change the base well performance when the surfactant is not included in the completion. To provide a better comparison, sensitivity analysis is done by normalizing the SASI-affected well performance to the base well performance on each reservoir property combination. This means a value of one implies that the addition of surfactant does not affect the well performance on that particular reservoir properties combination.

RESULT AND DISCUSSION

Four fluid systems on the Eagle Ford oil and rock system listed in Table 1 are tested through the whole workflow starting from laboratory measurement to the field-scale modeling. Results from each stage will be presented next using the color coding stated on the same table. In addition, laboratory experiment results in a Permian sample with five fluid systems listed in Table 2 are included as well to provide a quick investigation on the efficacy of SASI on other ULR. Color coding in accordance to the mentioned table will also be used to present the Permian results.

Interfacial Tension, Zeta Potential, Contact Angle, and Surfactant Adsorption Isotherm. Reduction of oil and water interfacial tension in the presence of surfactant is observed. The original IFT between Eagle Ford oil and water is measured to be 31.4 mN/m, which is a relatively high value compared to other oil that has been measured. This could be caused by the relatively lighter oil, reflected by the clear color of the crude oil as well as its relatively low density. The strongest IFT reduction is observed when 1gpt of Surf2 is added, reducing the value to 7 mN/m. Surf3 and Surf1 follow next with the IFT value of 10 mN/m and 17 mN/m, respectively, as presented by the left graph of Figure 1. A similar observation is observed on the oil sample from the Permian Basin as shown in the right graph of Figure 1. Native oil and water IFT of the Permian oil sample is measured to be 24.7 mN/m. In the presence of surfactants, lower IFT values in the range of 2 mN/m to 15 mN/m are observed.

It is also important to note that the extent of the IFT reductions observed in this study are not as significant as the typical reduction of surfactant flooding on a conventional reservoir. A lesser extent of IFT reduction is required for the capillary-driven imbibition mechanism as the magnitude of capillary pressure is linearly correlated as shown by the Young–Laplace's equation. However, higher IFT values could also reduce the production performance as relative permeability of oil and water is known to be inversely related to the IFT of the two phases.

Results from zeta potential measurements are given in the left graph of Figure 2. The magnitude of zeta potential of the three fluid systems consisting of surfactant are larger compared to the base case. This indicates that a more stable layer of water molecule is formed around the rock particle which can be translated into a more water-wet surface. The amphiphilic nature of the surfactant molecule allows an initially hydrophobic surface condition to have higher affinity to a water molecule by acting as a bridge between the surface and the water molecule. Surf1 is found to have the largest zeta potential value followed by Surf2 and Surf3. Based on this finding, Surf1 should also have the strongest wettability alteration capability when tested on the contact angle measurement, followed by Surf2 then Surf3. These results also agree with the experiment conducted with Permian rock samples, shown in the left graph of Figure 3. On this sample, it was observed that surfactants also increase the magnitude of zeta potential from the base.

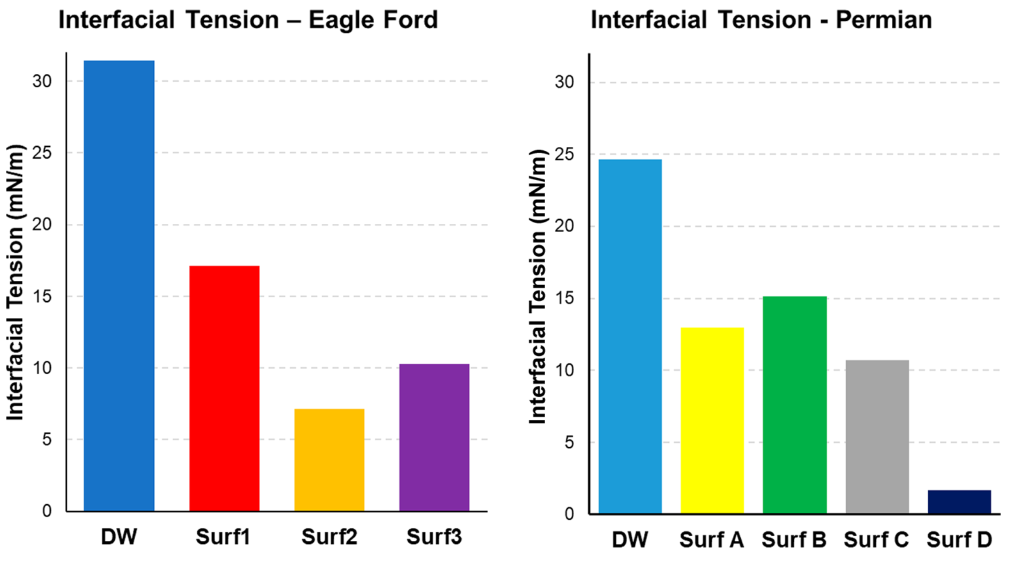

Figure 1. Interfacial tension measurement results of Eagle Ford (left) and Permian (right).

DOI: 10.1021/acs.energyfuels.9b00183
Energy Fuels 2019, 33, 6904–6920

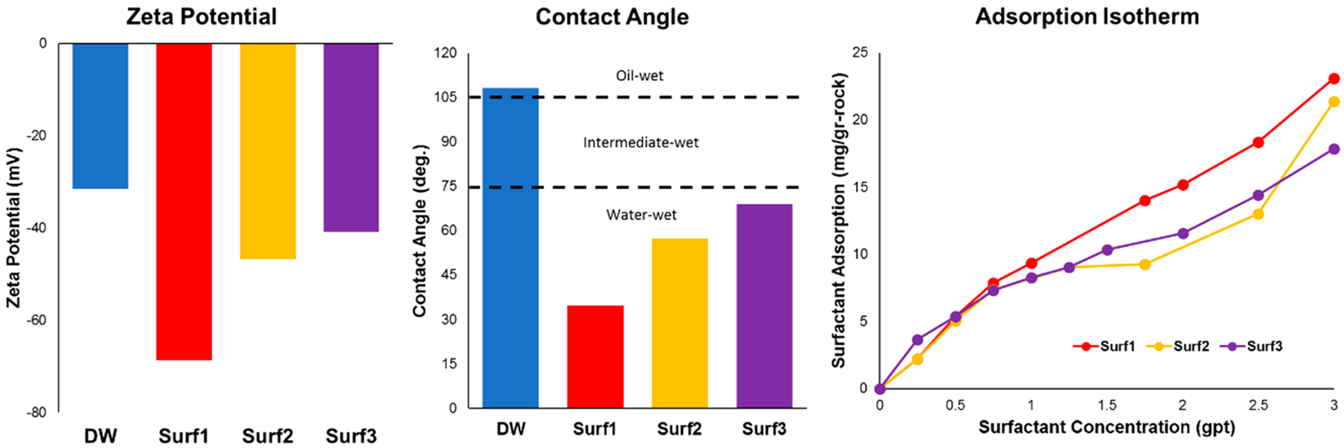

Figure 2. Zeta potential (left), contact angle (middle), and adsorption isotherm (right) measurement results of the Eagle Ford sample.

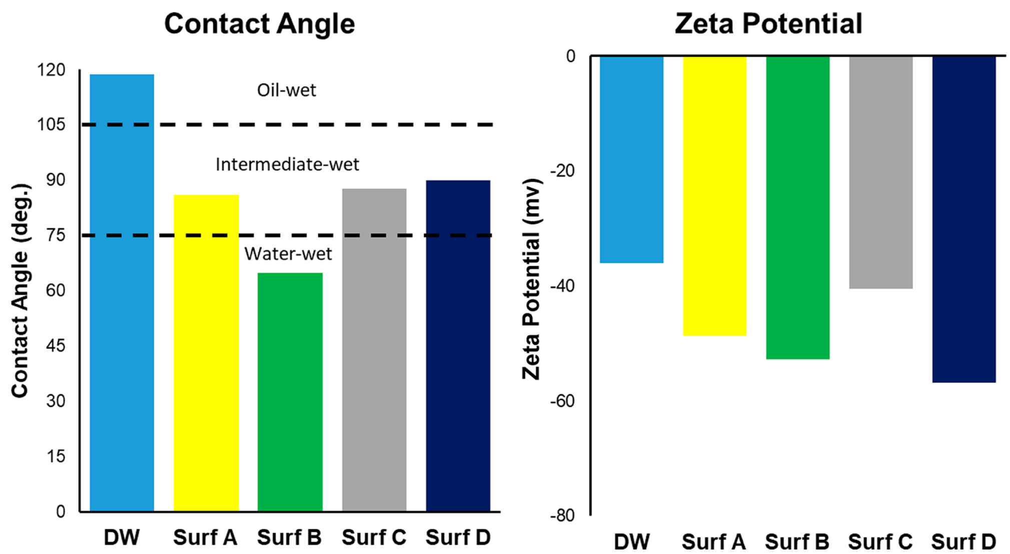

Figure 3. Zeta potential (left) and contact angle (right) measurement results for the Permian sample.

This verifies that the addition of surfactants helps to create a more stable water layer around the rock particle.

Consistent results are observed on the contact angle measurement as presented by the center graph of Figure 2. Initial wettability of the Eagle Ford falls in the oil-wet region, and the addition of surfactant alters the wettability to the water-wet region. As first estimated from the zeta potential measurement, Surf1 should have the most powerful wettability alteration property, which is supported by the contact angle measurement. From the same measurement, it can be concluded that Surf2 and Surf3 have weaker wettability alteration capability than Surf1. A similar phenomenon occurs with Permian rock samples, as its original wettability is a strongly oil-wet surface, but the wettability alteration is observed noticeably with the addition of surfactant, as displayed in the right graph of Figure 3. Compilations of pictures showing the oil drop structure as it contacts the Eagle Ford rock sample are shown in Figure 4. A significant difference is observed for an oil bubble formed when surfactant is and is not present in the solution. A more spherical shape is observed on the three bubbles formed in the presence of surfactant in the solution, providing clear, physical evidence of wettability alteration occurring under the influence of surfactant. As shown by the Young–Laplace capillary pressure equation, wettability is a dominant factor in determining the performance of SASI as it defines the direction of the capillary pressure.

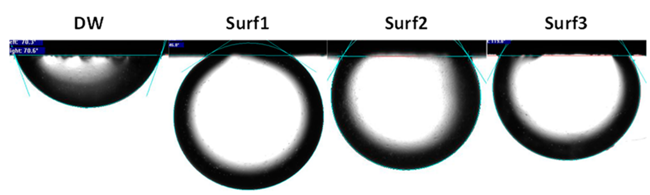

Figure 4. Comparison of oil drop curvature under the four fluid systems.

The surfactant adsorption isotherm serves as the weighting value for the capillary pressure and relative permeability curve modification on the modeling part of this work. Measurement is done by utilizing a UV–vis spectrophotometer which means that a calibration curve correlating light adsorption to the surfactant concentration as well as the specific wavelength of which such adsorption occurs must be determined first. Wavelength property as well as the calibration curve of each surfactant are determined previously which are then used in the measurement.[33] Adsorption isotherms of the three surfactants are compiled on the right graph of Figure 2.

DOI: 10.1021/acs.energyfuels.9b00183
Energy Fuels 2019, 33, 6904–6920

Comparing the three surfactants, Surf1 has the highest adsorption value compared to the two other surfactants on their corresponding concentration tested in this study.

In summary, a general trend can be observed from Figure 2 which contains zeta potential, contact angle, and adsorption isotherm results of the Eagle Ford sample. Surf1, which has the strongest wettability alteration as observed from the contact angle measurement, also possesses the largest zeta potential and adsorption, while the least wettability-altering surfactant, Surf3, has the lowest zeta potential value and adsorption isotherm. A pretty distinct trend can be observed that zeta potential, contact angle, as well as adsorption isotherm are all correlated to one another. Previous researchers have presented similar correlations on their data points.[20] This interconnection between the three properties is also highly essential as it shows that the modeling mechanism proposed in this work is valid and representative of the actual physics behind SASI.

Spontaneous Imbibition. The ultimate laboratory-scale performance evaluation of each fluid system is carried out through the spontaneous imbibition experiments. Cumulative oil production data are converted to recovery factor by normalizing the oil volume data to the OOIP of each core plug. Measurement of OOIP is done by converting the weight difference of the core after and before the aging process to volume with the help of density data. Recovery factor curves from all four imbibition experiments done are presented in Figure 5. The base case fluid system DW is observed to have the lowest recovery with the ultimate recovery factor of 4% OOIP. The recovery factor of the DW case is extremely low due to the oil-wet characteristic of the system which was shown from the contact angle measurement. Being in the oil-wet region, capillary pressure works against the oil production, hence the low recovery.

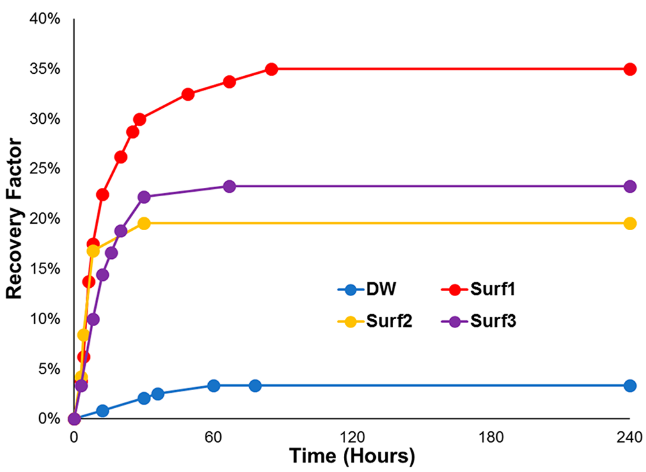

Figure 5. Oil cumulative recovery from the spontaneous imbibition experiment.

Addition of surfactant shows a positive impact as it increases the recovery factor of the spontaneous imbibition experiments. The original recovery factor of 4% on the base case is improved to 35% when Surf1 is added into the solution, 20% under Surf2, and 24% with Surf3. Comparing the imbibition results to the rest of the laboratory measurements, a correlation of CA and IFT to the imbibition performance can be observed. It was already determined before that Surf1 has the most water-wet wetting state, followed by Surf2, Surf3, and then DW. While for the IFT value DW has the highest IFT value, followed by Surf1, Surf3, and Surf2. Based on the Young−Laplace capillary pressure equation, reduction of IFT would cause a lower capillary pressure which should lead to a lower recovery factor. However, in the case of surfactant addition, IFT reduction is also accompanied by alteration of wettability to a more water-wet region. Wettability alteration would change the direction of capillary pressure to the positive sign, thus expelling more oil from the pore under the water-wet state compared to oil-wet.

Surf1 has the most hydrophilic wetting state as well as higher IFT compared to the other two surfactant fluid systems. Therefore, it is expected to also have the highest oil production as capillary pressure under this system would be large and in the direction that causes oil to be expulsed from the pore. Production recovery curves shown in Figure 5 verify the hypothesis where a recovery factor of 35% is observed when imbibition is run under Surf1. It is also important to note that this also supports the understanding that SASI is driven by capillary force, which the surfactant helps enhance by altering the direction of the force to produce more oil.

Incorporation of CT-scan technology was mentioned in a previous part; CT scanning is done multiple times throughout the whole experiment. Images from the CT machine are in the form of 3D reconstruction of each scanned core plugs. However, for presentation purposes, 2D snippets of the cross-sectional of each scan is made and presented instead of the 3D form. In order to be consistent, the position of each snippet is kept constant on every time step of the scan. Snippets then are grouped based on core plugs on each row and time step on each column as shown in Figure 6. Color grading is applied to the snippets to enhance the quality of the image. Brighter color represents higher density, while darker color represents lower density. The density value corresponds to the different fluid contained, and higher water contents would cause density to be higher than higher oil content as water has higher density compared to oil. Therefore, production of oil from the imbibition experiment as shown before should be reflected on the CT images with shift of color from dark to bright. As can be seen in the figure below, the expected change was observed. Fluid movement on the three surfactant cases are dominant on the horizontal plane. Horizontal movement could provide more evidence of the capillary-driven imbibition, and for the case of gravity-driven imbibtion, dominant color change in the vertical plane would be observed.

Laboratory-Scale Modeling. The next part of the study is the construction of the capillary pressure and relative permeability curves from the history-matching process of the laboratory-scale spontaneous imbibition experiment. The grid model of each core plug used in the experiment is constructed by converting CT images of each sample into the porosity map. The porosity grid model of the four core plugs is shown in Figure 7. As shown by the attached figure, the advantage of constructing the model through this procedure is the ability to incorporate the heterogeneity of the core plug sample. Once constructed, each plug model is placed in a water bath model for 10 days to simulate the Amott cell setup. Capillary pressure and relative permeability curves are obtained by comparing the oil recovery produced by the laboratory-scale model to the actual oil recovery data from the laboratory experiment. Both curves are generated manually and tested on the model. Curves with the closest match possible then are chosen.

DOI: 10.1021/acs.energyfuels.9b00183
Energy Fuels 2019, 33, 6904−6920

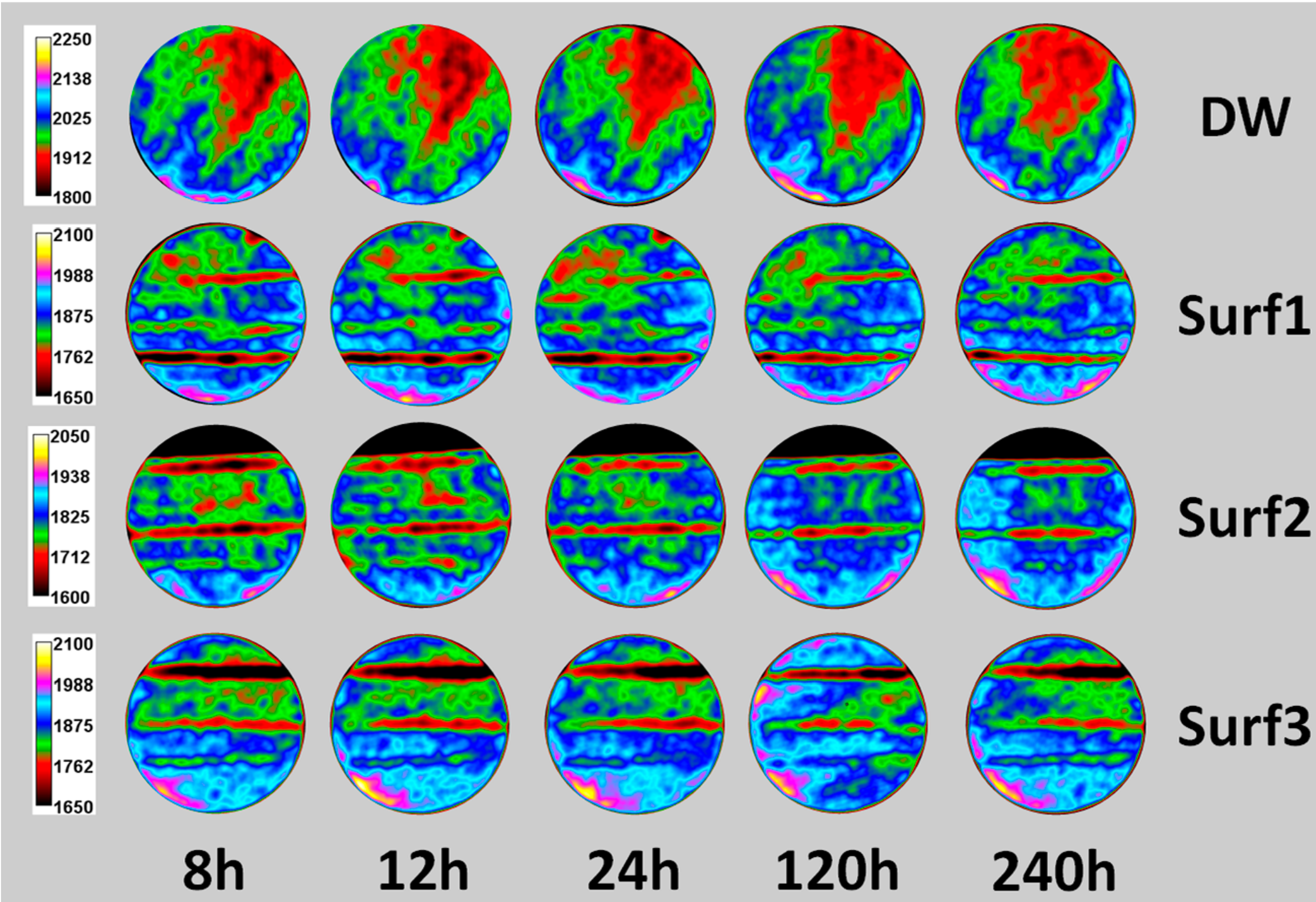

Figure 6. CT snippets on different timesteps of each core plugs tested under imbibition experiment.

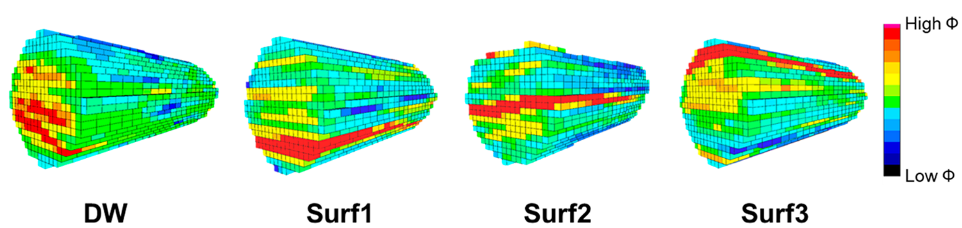

Figure 7. Porosity grid model of the laboratory-scale model.

History-matching results are presented in Figure 8, with triangle points showing experimental data and solid lines representing numerical results. The capillary pressure and relative permeability curves resulting in the production data shown in Figure 8 are presented in Figure 9. Although the contact angle measurement for the DW case results in negative value of Young−Laplace capillary pressure, capillary pressure is still observed on the curve as oil production is still observed on the laboratory experiment. This could be caused by the presence of some water-wet mineral in the core sample that allows for some imbibition to occur. From Figure 9 it can also be seen that generally the addition of surfactant alters the capillary pressure curve in two ways. First, it reduces the maximum capillary pressure as an effect from the reduction of IFT. Most importantly, it also shifts the intersection point of the curve on the x-axis ($S_w(P_c = 0)$) to the right which causes larger capillary force to act in the pore, and as a result, higher oil recovery factor is obtained. It is also found that this $S_w(P_c = 0)$ variable is closely related to the contact angle of each system where lower contact angle value results in higher $S_w(P_c = 0)$ and vice versa. Relative permeability of water and oil is also

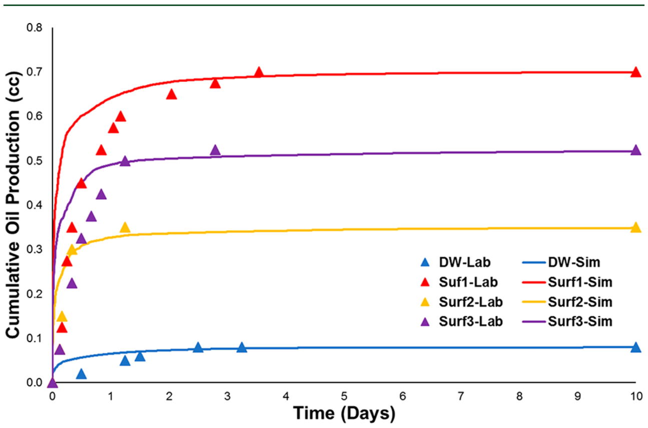

Figure 8. Laboratory and numerical model production data.

DOI: 10.1021/acs.energyfuels.9b00183
Energy Fuels 2019, 33, 6904−6920

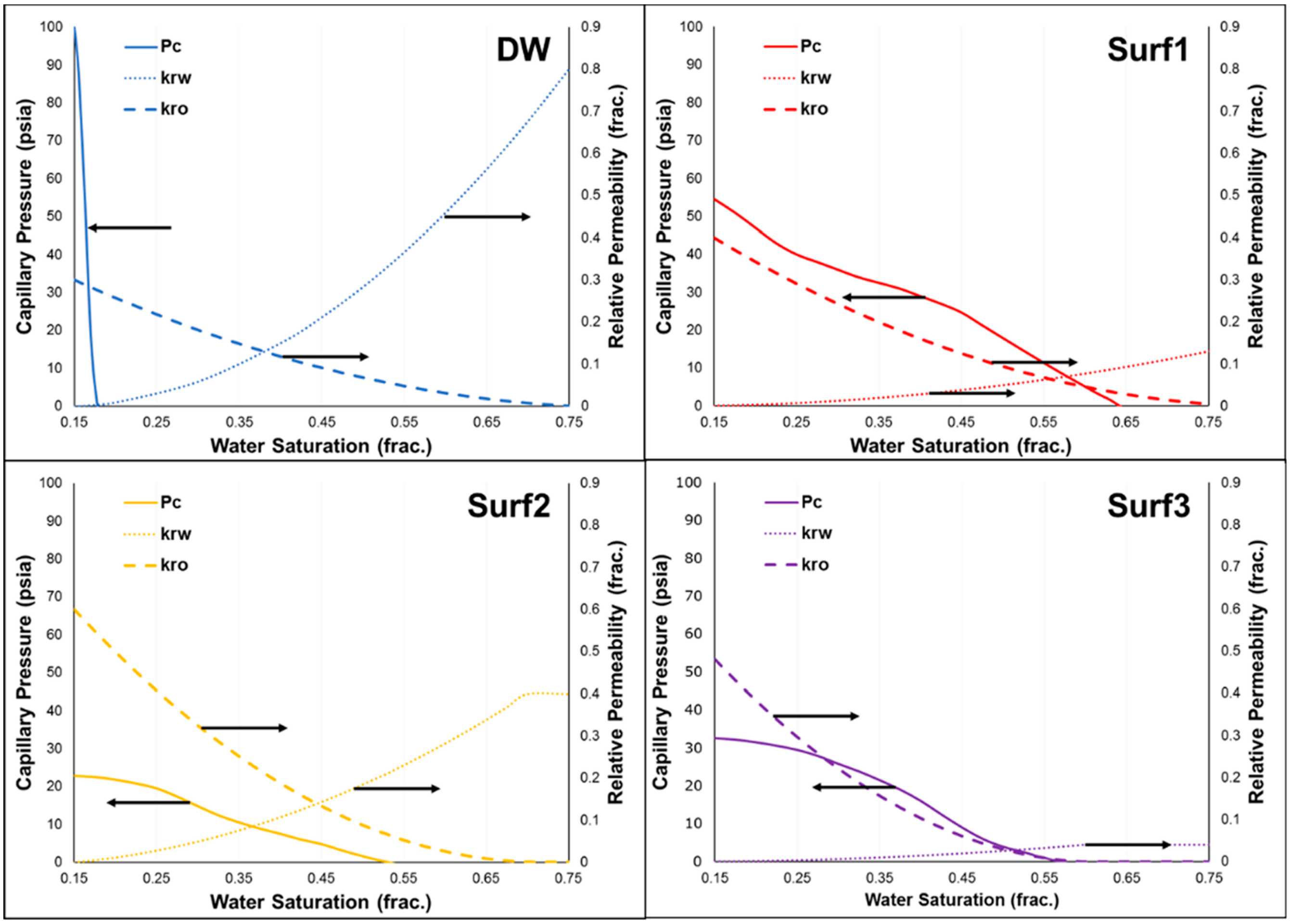

Figure 9. Capillary pressure and relative permeability curves of all four fluid systems.

affected by the presence of surfactant. On a more hydrophilic surface, maximum relative permeability of water is reduced which could be caused by the stronger affinity of the rock surface to the water molecule, hindering the movement of the water in the pore. Accordingly, maximum relative permeability for the oil would be increased on the same rock, as the rock surface has less attraction to the oil molecule which allows for a better flow of the oil. With the exceptionally small size of the shale pore space, this phenomenon could have a more significant impact as the water and oil molecule would move in a closer distance to the surface of the pore.

Field-Scale Modeling. One of the final goal of this study is to investigate the effect of SASI on the field scale. Adsorption isotherm, capillary pressure, and relative permeability curves obtained from the laboratory-scale section are applied on a synthetic dual-porosity field numerical model which will provide an insight on the efficacy of SASI on a field application. In this study, the efficacy of each fluid system is analyzed by investigating three main key points of the well production data: oil production rate, cumulative oil production, and cumulative water production. Data of the three variables from all four fluid systems are presented in Figure 10. Color coding of each fluid system as previously defined by Table 1 is still applied on the figure. Solid lines on the figure represent oil production rate, while dashed and dotted-dashed lines represent cumulative oil production and cumulative water production, respectively.

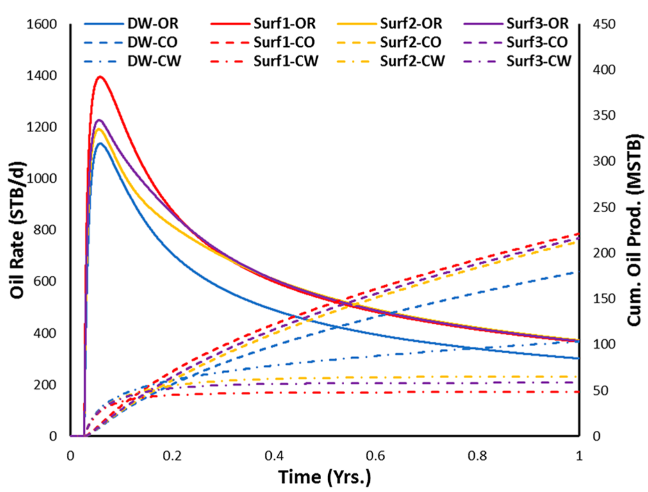

Figure 10. Well-scale numerical model results of SASI application.

Peak oil rate from the base case is observed to be 1100 STB/d with the 3-year cumulative oil production of 335 MSTB. Field-scale modeling shows that the addition of surfactant enhances the production of oil by improving both peak rate and cumulative oil. The highest production improvement is observed from Surf1 which improves the peak rate and cumulative oil by 23% and 18% from the base case, respectively. Surf2 and Surf3 also provide additional recovery with the increment of peak rate by 16% and 17% and

DOI: 10.1021/acs.energyfuels.9b00183
Energy Fuels 2019, 33, 6904−6920

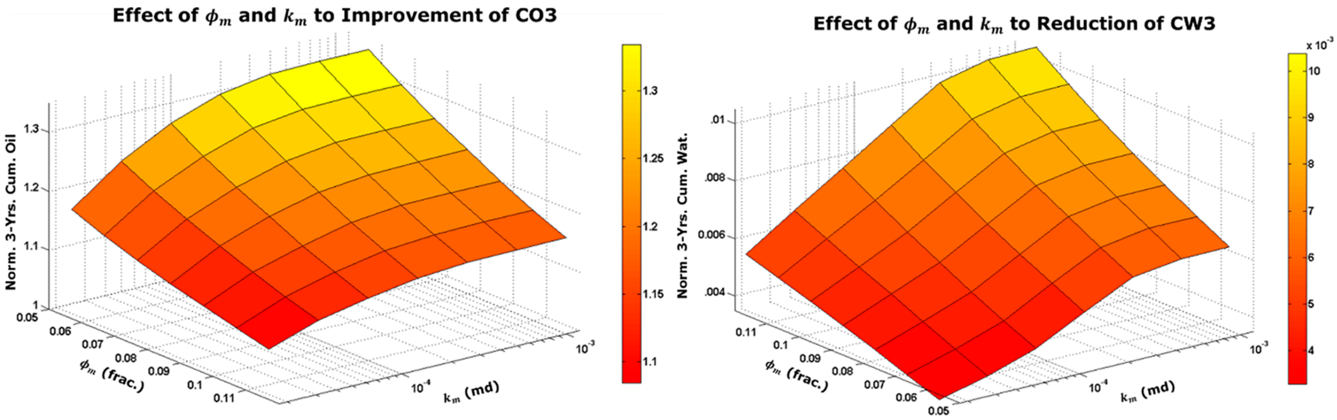

Figure 11. Effect of ϕ_m−k_m to 3 years. Cumulative oil improvement (left) and water reduction (right).

increment of cumulative oil recovery by 5% and 8%, respectively. From this result, it can be concluded that the result observed from the laboratory-scale studies translates to the field scale. The improvement of oil recovery caused by surfactant addition observed on the laboratory-scale investigation is also observed on the field scale. The field-scale result shows that Surf1 provides the highest improvement of recovery which is also shown by the laboratory-scale studies. However, it can be clearly perceived that the level of production improvement on this field-scale model is not as significant as the laboratory-scale studies. On the laboratory-scale study, incremental cumulative oil recovery attains as high as 300% of the base case, while for the field-scale model, the highest cumulative oil improvement calculated is 18% of the DW base case. This discrepancy can be explained by the absence of pressure drawdown effect on the laboratory-scale studies, which is one of its main limitation. Pressure drawdown given by the well in a real life scenario causes oil to expand and be produced out of the reservoir. This production mechanism is not modeled on the laboratory-scale testing as no pressure difference is applied on the imbibition experiment. When the primary recovery mechanism is added, it can be observed that the effect of capillary-driven imbibition to the total production is masked by the production from the pressure drawdown. A similar observation was also found on the upscaling work shown in other publications.[10,15]

In applying a laboratory-tested production enhancement method to the field scale, some interesting observations of the production enhancement mechanism are often waiting to be discovered. For the case of SASI, one example is the mechanism of peak oil rate improvement by the addition of surfactant in the completion. Taking a closer look at the change of oil saturation distribution on the whole reservoir grid model, a dominant fraction of the oil transfer from the matrix to the fracture system occurs during the shut-in period. Naturally, the oil transfer from the matrix to the fracture is also accompanied by the transfer of water from the fracture to matrix. As explained before, this study assumes that surfactant is added as a completion fluid, meaning that it would only be present in the fracture system in the reservoir at the start of the simulation run. The transfer of water from the fracture to the matrix would also bring surfactant into the matrix grid. Surfactant then improves the capillary pressure which causes more oil to be expelled or transferred to the fracture system. It is observed that when pressure drawdown is applied to the well after the shut-in process the peak oil production rate is highly dependent on the amount of oil transferred to the fracture system. Therefore, it can be concluded that the improvement of capillary pressure by the addition of surfactant molecule possesses the ability of improving initial production of the well by enhancing the matrix-fracture oil transfer during the shut-in period.

Another important observation in the comparison of the four tested fluid systems is that water production on the surfactant cases is significantly less than the base case. It can also be seen that Surf1 which has the highest oil recovery factor also produces the least amount of water. Enhancement of oil production through SASI is caused by the capillary-driven expulsion of oil, which naturally is also accompanied by the intake of water into the matrix. Therefore, higher oil production would mean more water to be trapped inside the matrix, which translates into less water being produced on the surface. Reduction in water production is not one of the effects observed in the laboratory-scale study of SASI. However, it could be one of the most favored effects. Although water production is not an issue in the Eagle Ford reservoir where this study is mostly focused, the Permian basin is definitely a contrast, where water production generates a noteworthy problem due to its high volume.

Sensitivity Analysis. One of the objectives of this study is to construct a comprehensive workflow in assessing the performance of surfactant to increase the oil production of a shale oil well through SASI mechanism. With the completion of the field-scale model section of this study, this objective is fulfilled. The next step of this study is to investigate the effect of reservoir characteristics and completion parameters on the efficacy of the surfactant on a field-scale application. Previous study has reported a sensitivity analysis study by applying a range of values for matrix and natural fracture porosity and permeability to a field-scale model implementation of SASI.[33] Based on their study, less improvement of initial oil recovery was observed when higher matrix porosity is applied to the model. In addition, smaller differences in surfactant performance between all surfactants included in the work were also observed in higher porosity values. Increasing fracture porosity improves the production enhancement in terms of rate and cumulatively with performance differences between surfactants also moving further apart from each other. Fracture spacing was also considered as an important parameter and was found to significantly affect the performance of the surfactant. Closer spacing resulted in increased well performance enhancement due to SASI.

DOI: 10.1021/acs.energyfuels.9b00183
Energy Fuels 2019, 33, 6904−6920

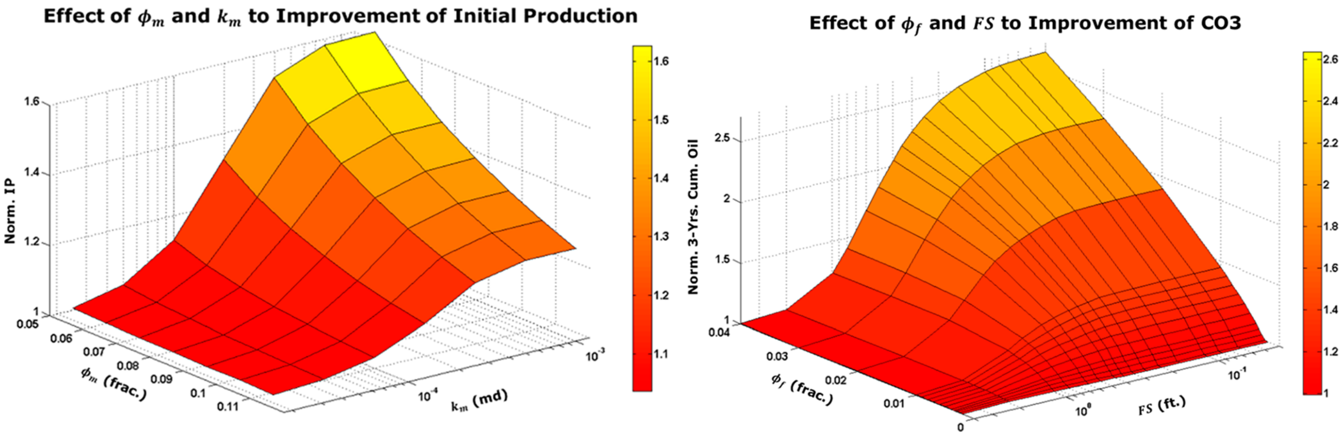

Figure 12. Effect of ϕ_m−k_m on initial production (left) and ϕ_f−FS to 3 years cumulative oil (right) improvement.

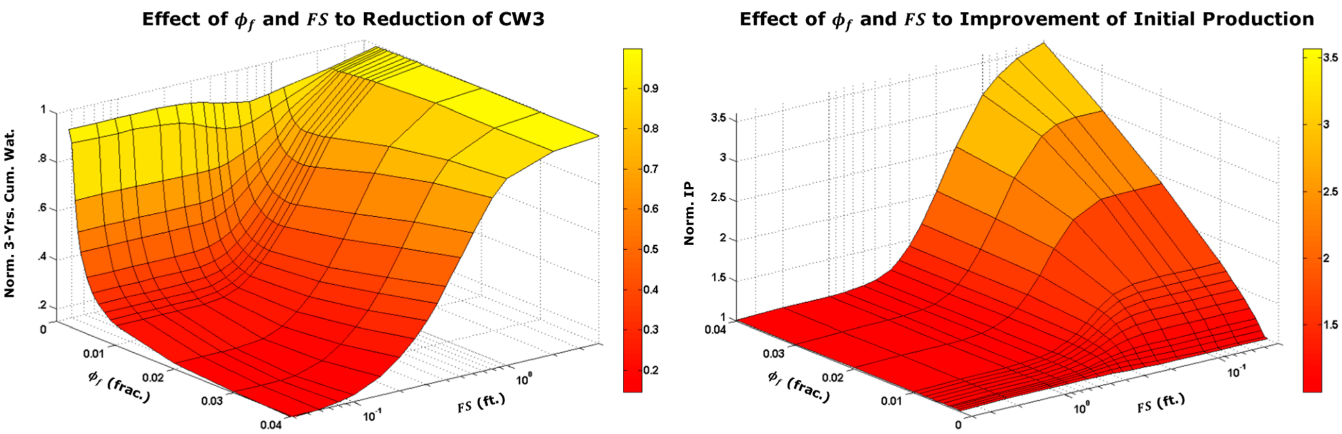

Figure 13. Effect of ϕ_f−FS to 3 years cumulative water reduction (left) and initial production improvement (right).

The following section will cover a more in-depth sensitivity analysis done in continuation of the work mentioned earlier. Matrix porosity and permeability, fracture porosity, permeability, spacing, surfactant concentration, and shut-in time are adjusted as control variables with cumulative oil, water, and initial oil rate as dependent variables. Surf1 is chosen as the surfactant in this analysis as it is the best performing surfactant in this study. In this study, the result of the sensitivity analysis is presented after normalization to the base case of each reservoir property. Peak oil rate (Initial Production or IP), cumulative oil production (CO3), and cumulative water production (CW3) on each combination of reservoir properties are presented after being normalized to the IP, CO3, and CW3. The sensitivity ratio of one implies that the surfactant does not affect the production of the well as the production of the well is identical on both the surfactant and base case. It is also important to note that all sensitivity results are presented in the form of a 3-axis graph to provide a more comprehensive analysis on the effect of each coupled property on the efficacy of surfactant treatment.

The effect of matrix porosity and permeability on the three-year cumulative oil improvement and water reduction are presented in Figure 11. It can be observed that both lower matrix porosity and higher matrix permeability result in a more effective SASI application as higher CO3 as well as a greater reduction in CW3 are observed. On the left graph of Figure 12, higher improvement of initial oil production rate from SASI is observed on the combination of low porosity and high permeability values. The effect of porosity values is also observed to be more significant on higher values of permeability, and a similar observation is observed on the effect of permeability. Better surfactant performance on lower porosity values is caused by less production from the primary recovery. This is due to lower amount of oil being available in the pore space, making the production from surfactant-induced capillary force more dominant. From the capillary pressure curve, it can be comprehended that capillary-driven oil recovery is a function of oil saturation and is independent of the actual volume of oil available. This translates to the conclusion that SASI is highly effective on low porosity and permeability values. The reduction of water production accompanying improvement of oil production also indicates that capillary force is the cause of the production improvement. Capillary imbibition occurs in the form of oil and water exchange from the fracture to the matrix system. Higher intake of the volume of water into the matrix by capillary imbibition explains the reduction of water production. It can be safely concluded that SASI is highly effective in improving cumulative oil production on a reservoir with low porosity value.

Fracture porosity and spacing are modified, and their effect on IP, CO3, and CW3 are presented on the right figure of Figure 12 and Figure 13. Larger fracture porosity results in a more effective surfactant performance, as shown by the higher improvement of both IP as well as a more significant decrement in CW3. This result is caused by the initialization

DOI: 10.1021/acs.energyfuels.9b00183
Energy Fuels 2019, 33, 6904−6920

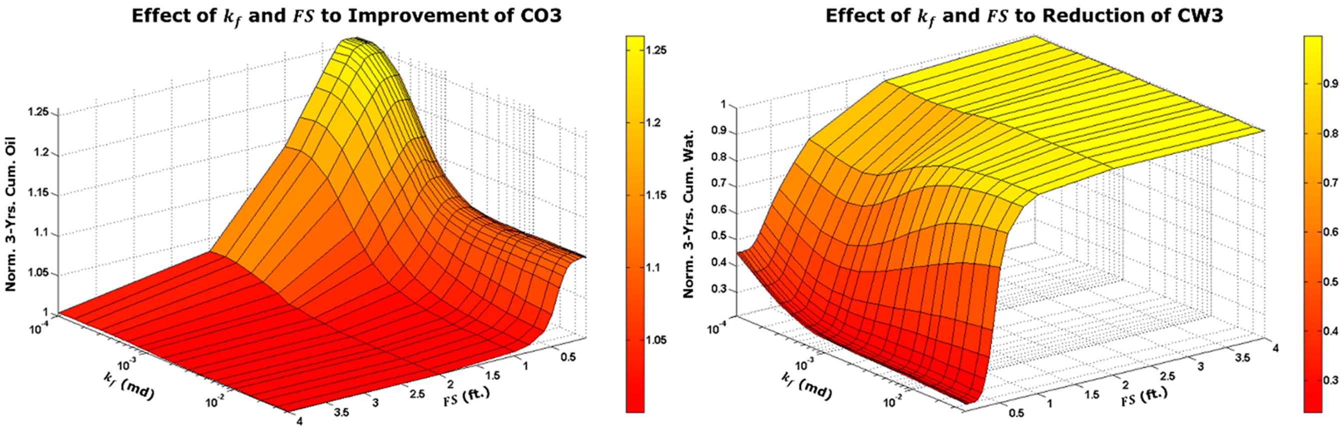

Figure 14. Effect of k_f–FS to 3 years cumulative oil improvement (left) and cumulative water reduction (right).

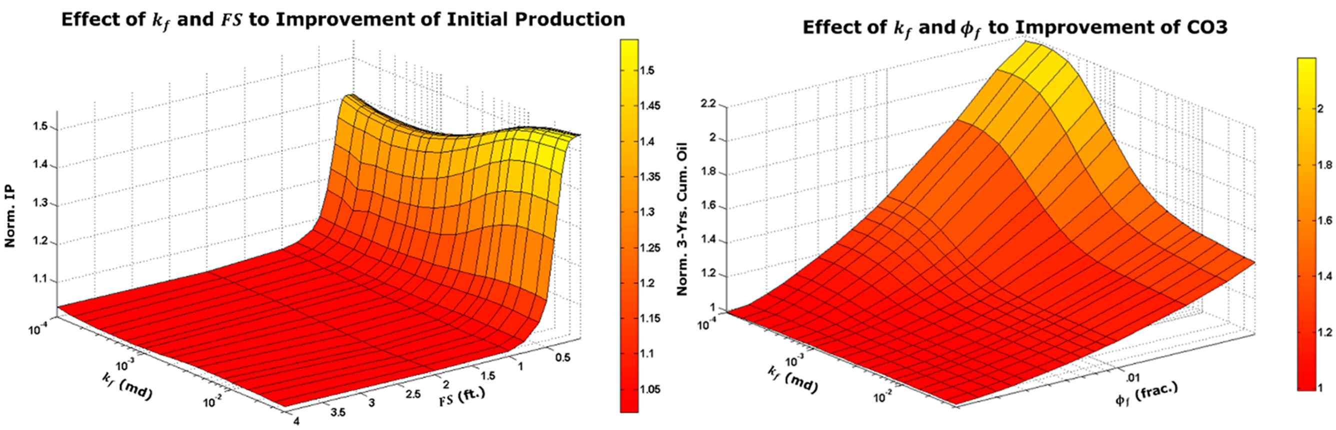

Figure 15. Effect of k_f–FS on initial production improvement (left) and k_f–ϕ_f 3 years cumulative oil improvement (right).

of the field-scale model which is set by setting the surfactant molecule to be existing only in the fracture system. Higher values of fracture porosity mean a larger fracture volume. A larger fracture volume then would mean that more surfactant exists in the reservoir. Greater amounts of surfactant allow for more imbibition to occur, and as reflected in the sensitivity study, better improvement of oil recovery is observed.

Fracture spacing is defined as the distance between two adjacent fracture systems. Smaller spacing value indicates a reservoir that has high fracture density with smaller distance between each fracture. It was defined before that SASI works through the improvement of matrix–fracture transfer of oil and water. Therefore, spacing between fractures should have a significant impact on the efficacy of SASI on a field-scale application. Affirming the statement, larger values of fracture spacing are observed to reduce the impact of surfactant on oil and water production. Fractures being more distant from one to another would increase the amount of pressure needed to move oil from the matrix to the fracture, hence lower improvement of oil recovery by SASI. It is can also be seen that fracture spacing has a more significant impact on the improvement of IP than CO3 as the onset of the curve on the right figure of Figure 15 occurs far more to the right compared to the onset of the curve on the left figure of Figure 14. This observation indicates that the long-term effect of SASI is less affected by the quantity of fracture spacing.

Combining the two control variables, both porosity and spacing of the fracture affect the surfactant performance. However, it can be seen that fracture spacing has a more dominant effect on the efficacy of SASI application. A similar trend is also observed when comparing the effect of fracture permeability and spacing to the effectivity of SASI in improving the oil production of the well. As seen in Figure 14 and the left figure of Figure 15, a more apparent change in the production enhancement is observed along the fracture spacing axis. More dominant effect of spacing than porosity supports the statement that SASI would show a more significant production enhancement when it is applied on a reservoir with higher number of fracture systems present.

Going back to the sensitivity analysis on the fracture permeability, a negative correlation between improvement of CO3 and the reduction of CW3 to the fracture permeability is observed. In addition, a plateau is also observed on higher permeability. To explain this trend, the effect of fracture permeability on improvement of IP must be analyzed first. Higher fracture permeability value results in a greater increment of initial production rate. Fracture permeability is closely related to the matrix–fracture transfer function where higher fracture permeability results in a more significant fluid transfer between the two systems. As mentioned before, field implementation of SASI results in higher well performance due to the higher volume of water imbibition from the fracture to the matrix. Water intake into the matrix consequentially must be accompanied by the expulsion of oil. Since better fracture permeability correlates to better fluid transfer between the fracture and the matrix, this results in more imbibition occurring in the reservoir. A fracture system with higher volume of oil present would have higher IP as this early time

DOI: 10.1021/acs.energyfuels.9b00183
Energy Fuels 2019, 33, 6904–6920

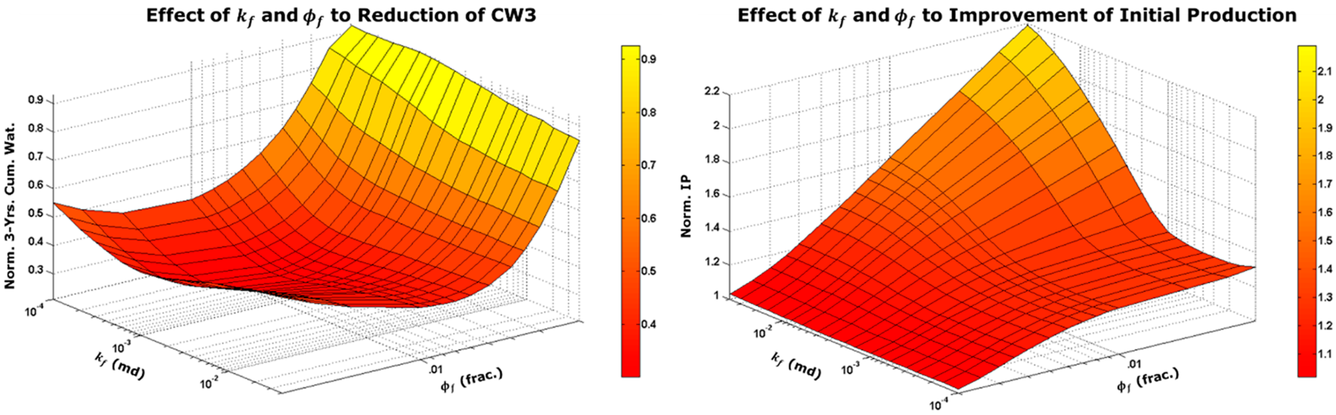

Figure 16. Effect of k_f–FS on initial production improvement (left) and k_f–ϕ_f 3 years cumulative oil improvement (right).

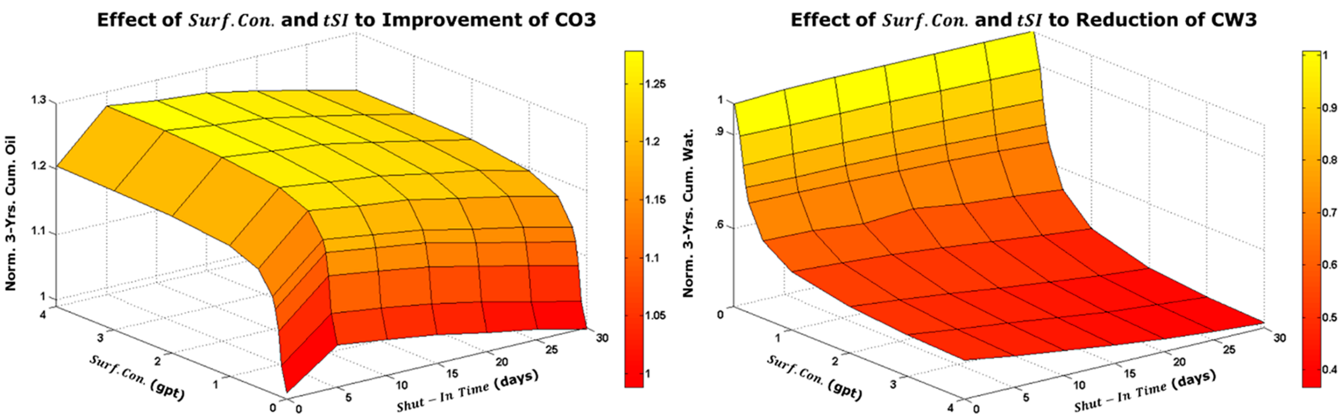

Figure 17. Effect of Surf.Con.−tSI on 3years cumulative oil improvement (left) and cumulative water reduction (right).

production is a result of oil production from the fracture. On the other side, as more oil is transferred into the fracture, it is noted that less oil volume is left in the matrix. CO3 is a function of the oil volume in the matrix due to the primary recovery mechanism of oil expansion. Therefore, the observation where higher IP is noted to occur in combination with lower CO3 is somehow logical. The plateau observed on higher fracture permeability value of Figure 14 can also be explained by the explanation provided before, that expected lower CO3 improvement is complemented by the higher IP at those high fracture permeability values.

The combination of the fracture permeability and porosity effect on the performance of surfactant is presented on the right figure of Figure 15 and Figure 16. Enhancement in CO3 by SASI is the highest when minimum fracture permeability is applied in combination with higher value of fracture porosity, while on the enhancement of IP, SASI performed the best improvement on the reservoir with both low value of fracture permeability and porosity.

The next part of the sensitivity analysis is highly beneficial as both control variables can be a part of the design on an actual field-scale application of SASI. A range of surfactant concentrations and shut-in times are tested in the field-scale model with the results presented in Figure 17 and Figure 18. As usual, the base case of no surfactant and no shut-in time is used as the normalization factor to all of the cases. All reservoir properties are kept constant on all cases run to isolate the effect of surfactant concentration and shut-in time on production enhancement. Looking at the CO3 result, it is clearly shown that the addition of surfactant improves the

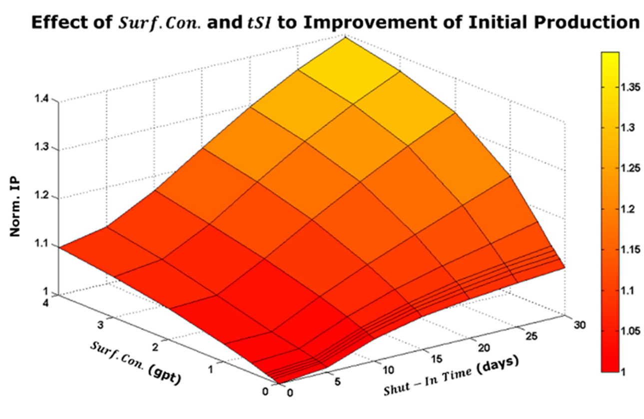

Figure 18. Effect of Surf.Con.−tSI on initial production.

performance of the well significantly. Steep inclination in improvement of cumulative recovery is observed when surfactant concentration is increased from 0 gpt to 1 gpt, followed by a more gradual increment when higher surfactant loading is applied. Shut-in time is found to play an important role in the improvement of CO3 as well. Adding shut-in time from 0 to 5 days results in a significant addition of oil recovery, and increasing surfactant concentration amplified the recovery increment. However, when shut-in time is elongated up to 30 days, the improvement of cumulative oil is observed to decrease. Before providing an explanation of this phenomenon, it is necessary to go over the effect of concentration and shut-in time on cumulative water and initial oil rate. Increasing

DOI: 10.1021/acs.energyfuels.9b00183
Energy Fuels 2019, 33, 6904−6920

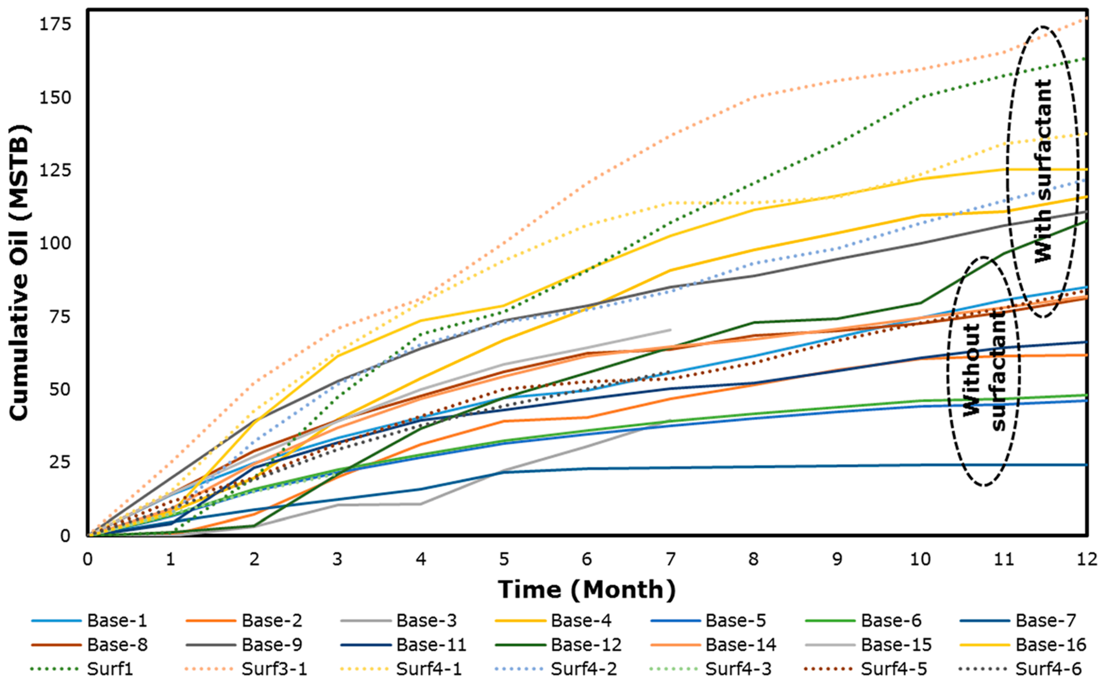

Figure 19. Actual cumulative oil recovery through time of Stack X and Stack Y.

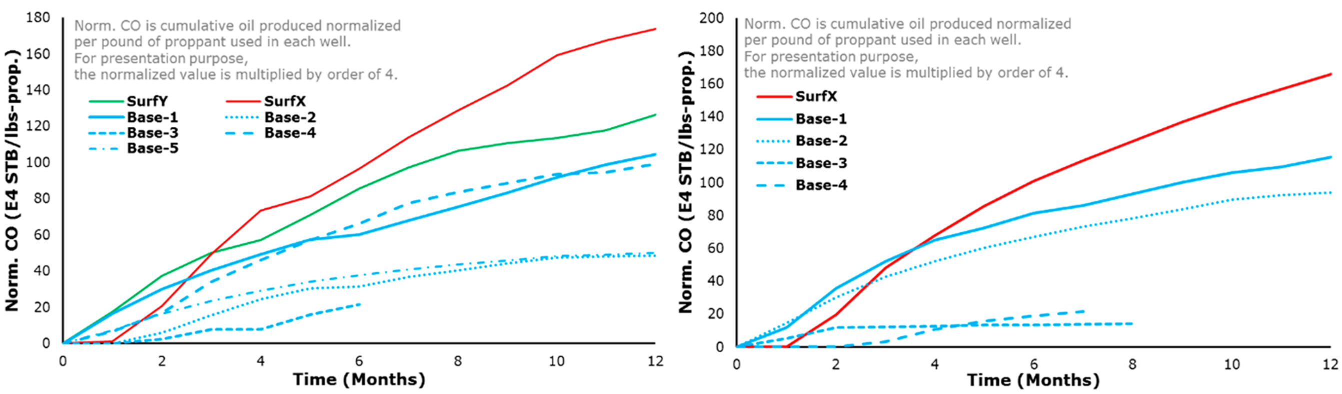

Figure 20. Field data of Stack X (left) and Stack Y (right) well-to-well oil production comparison.

surfactant concentration and shut-in time reduces further the CW3 with similar slope change observed on the CO3. Initial production rate follows a similar trend to the CW3 where increasing concentration and shut-in time cause an even higher improvement of IP. Comparing the three responses, a disparity in the trend of CO3 to both CW3 and IP rate is observed. The addition of concentration and shut-in time is observed to improve both cumulative water reduction and initial production, while the same trends are not observed on the cumulative oil. It is believed that the reasoning of this discrepancy is similar to the explanation of the riveting trend observed on the sensitivity analysis done on fracture permeability. Reduction of cumulative oil is caused by a larger volume of oil transferred to the fracture system. This theory is supported by the fact that water production is low on the same concentration and shut-in time value where cumulative oil is lower than a shorter shut-in time, which shows that imbibition still occurs.

Based on the sensitivity analysis of surfactant concentration and shut-in time, it can be concluded that larger surfactant concentration could lead to higher well performance and is not observed to cause any damage to the production. However, economics must be taken into account as the law of diminishing return also applies in this mechanism. Shut-in time is also determined to be beneficial as it allows for more SASI to occur, improving oil recovery, reducing cumulative water, and increasing initial production rate. Optimum shut-in time is also another important factor to be investigated as longer shut-in time could have lower cumulative oil recovery than shorter shut-in time.

Actual Well-to-Well Comparison. As a final part of this work, actual oil production data from field-scale implementation of SASI are presented in Figure 19 and Figure 20. Raw data of cumulative oil production from 21 wells are given in Figure 19. Base cases of no surfactant injected are presented as solid lines, while for wells with the addition of surfactant in their completion fluid, their cumulative oil data are presented as dotted lines. Generally, it can be seen that the cumulative oil data from dotted lines are grouped around higher value compared to solid lines. This result indicates that the addition of surfactant does improve the performance of these wells. However, utilizing raw production data in a comparison study

DOI: 10.1021/acs.energyfuels.9b00183
Energy Fuels 2019, 33, 6904−6920

could be misleading due to the possibility of different completion configurations on each well. Therefore, to further explore this field-scale result, a normalization study is needed.

Study in this form is essential as it shows an actual outcome on the application of SASI on the field scale. However, in addition to its representability, a real-life case study is also highly complicated as each well is different from reservoir, completion, and production points-of-view.

Therefore, in this study, wells are selected carefully to eliminate any other variable that could impact the production of each well aside from the addition of surfactant. Wells incorporated in the two figures are wells from a single operating company. This first filter is highly important as companies are known to have different regulations and rules-of-thumb that they apply to their wells. A total of 12 wells are selected and divided into two different graphs to eliminate the effect of dissimilar reservoir properties as they are added from two different stacks, Stack X and Stack Y. After all of these filters and selections are applied, a final normalization step is done. To eliminate the effect of completion size on the oil production of each well, each oil production is normalized to the amount of proppant used. Then for presentation purposes, the final normalized value is multiplied by 10^4.

Well comparison from Stack X is presented on the left figure of Figure 20, while the right figure presents the comparison on Stack Y. It can be observed that on Stack X production of oil from the surfactant-treated well is observed to be higher than all other 5 base cases with similar results observed on wells producing from Stack Y. Enhanced oil production performance observed on these actual wells confirmed that the positive results shown in multiple laboratory studies previously published are applicable on the field scale. It is natural for the next part of this field data case study to be continued with economical assessment of SASI, an assessment on whether the application of the method is economically feasible or not. However, due to the limitation of the public data available, such analysis is not included in the scope of this work. Nonetheless, this field case example proves that the field application of SASI successfully improves oil production of those wells with surfactant added as part of their completion fluid.

■ SUMMARY

These core samples are unconventional in the sense that we can no longer saturate with brine to 100% aqueous phase saturation followed by standard drainage to S_{wi} followed by imbibition from S_{wi} to S_{or} when the capillary pressure reaches zero. The inability to directly pump fluids into these rocks on a reasonable time scale and perform standard saturation cycles implies that standard or special core analysis as we know it is no longer feasible. Mother Nature has made it such that the oil-wet propensity of these rocks allows oil to gradually soak into core samples until we attain oil saturations in the range of 70−80%. We know this because we constantly CT scan the cores during the natural soaking in oil until we no longer observe changes in CT numbers. This averages 2−3 months. We recognize that the inability to attain irreducible water saturation is a weakness. However, even with such obstacles we have been able to demonstrate the role of surfactant additives in the aqueous phase.

The research presented along with the field results clearly indicate the necessity of utilizing surfactants for completion. We present data from the laboratory that show a good correlation between static contact angles measured on chips that have been retrieved from reservoir intervals and recovery factor from static imbibition experiments from core plugs saturated with reservoir crude oil. Proper aging of the sample in crude oil at reservoir temperature followed by immersion in surfactant solution results in wettability alteration from oil-wet to water-wet. As this occurs, the calculated imbibition capillary pressure goes from a negative to positive value as the measured contact angle of the aqueous phase covers a range from ∼120° (oil wet) to less than 90°(neutral wet) and, as observed, can reach values as low as ∼30° (water wet). It follows logically from this observation that capillary pressure as determined by the Young−Laplace equation should also correlate to imbibition measurements. We demonstrate that the relation between capillary pressure and recovery due to imbibition indeed correlates strongly. This has been achieved by careful measurements of imbibition in multiple core samples from multiple reservoirs with a range of baseline wettability. We believe alteration of imbibition capillary pressure and improvement of oil relative permeability adequately represent the physical mechanisms observed from lab results, thereby justifying our history matching and upscaling techniques. The methodology presented in this manuscript along with previous research put us in the position to upscale lab results into meaningful numerical simulation to demonstrate the efficacy of surfactants. The field results aptly demonstrate the potential of SASI that operators with significant acreage positions would be remiss to discount or ignore without proper due diligence.

■ CONCLUSION

1. Addition of surfactant into an oil/water/rock system reduces the IFT of oil and water. However, it is important to note that the degree of IFT reduction observed in this work is far less than surfactants designed for conventional surfactant flooding.
2. Addition of surfactant alters the wettability of the rock surface from the original oil-wet condition to water-wet as determined by static contact angle measurements.
3. Addition of surfactant tends to stabilize the water layer wetting the rock surface as observed by generally increasing magnitude of the zeta potential.
4. Laboratory-scale imbibition experiment shows improvement of oil recovery by addition of surfactant as a result of wettability alteration.
5. Contact angle, zeta potential, and surfactant adsorption measurements tend to correlate with wettability alteration.
6. Static contact angle alone correlates well with recovery factor observed in SASI experiments.
7. Capillary pressure calculated from IFT, contact angle, and petro-physical properties of the rock also correlates well with recovery from SASI experiments.
8. Increasing capillary pressure and relative permeability allow history matching of core-scale numerical simulation from low recovery with water imbibition alone to higher imbibition recovery with the addition of surfactant.
9. Reservoir properties such as matrix and fracture porosity and permeability have a significant effect on the results of field-scale simulation of SASI as observed in upscaled dual porosity simulation. Better characterization of

DOI: 10.1021/acs.energyfuels.9b00183
Energy Fuels 2019, 33, 6904−6920

hydraulic and natural fractures is key in improving SASI design.
10. Upscaling the numerical simulation to field dimensions with the capillary pressure and relative permeability shows SASI improves the initial oil production rate by 22% and 3 year cumulative oil recovery by 18.4% when compared to the base case with no surfactant.
11. Field results show even better recovery performance than the best case simulations presented in this work.

AUTHOR INFORMATION

Corresponding Author

*E-mail: rakananda_saputra@tamu.edu.

ORCID

I Wayan Rakananda Saputra: 0000-0001-6319-2319
Fan Zhang: 0000-0001-9839-5597

Notes

The authors declare no competing financial interest.

ACKNOWLEDGMENTS

The authors would like to thank Crisman Institute for Petroleum Research for funding this research as well as ConocoPhillips and Pioneer Natural Resources for their contribution in providing samples for the experimental study. We also would like to express our gratitude to Johannes Alvarez, Randy Ardywibowo, John Maldonado, Rodolfo Marquez, and Claire DeCuir for their help in various parts of the work.

NOMENCLATURE

ϕ_f = Fracture porosity
ϕ_m = Matrix porosity
AFM = Atomic Force Microscopy
CA = Contact angle
CA_m = Measured contact angle
CT = Computed topography
CO3 = 3-years cumulative oil recovery
CW3 = 3-years cumulative water recovery
frac. = Fraction
ft = Feet
FS = Fracture Spacing
g/cm^3 = Gram per cubic centimeter
gpt = Gallon per thousand gallon
θ = Contact angle
IFT = Interfacial tension
IP = Initial oil production rate
k_m = Matrix permeability
k_f = Fracture permeability
k_{ro} = Oil relative permeability
k_{rw} = Water relative permeability
md = Millidarcy
mg/g-rock = Milligrams of surfactant per grams of rock
mg-KOH/g-oil = Milligrams of potassium hydroxide per grams of oil
mN/m = Millinewton per meter
MSTB = Thousands of stock tank barrel
mV = Milivolt
nd = Nanodarcy
nm = Nanometer
OR = Oil Production Rate (STB/d)
Pc = Capillary pressure
Pc_{max} = Maximum capillary pressure
r = Pore radius
σ = Interfacial tension
$S_w(Pc = 0)$ = Water saturation of zero capillary pressure
S_{wi} = Initial water saturation
S_{or} = Residual oil saturation
SASI = Surfactant-Assisted Spontaneous Imbibition
STB/d = Stock tank barrel per day
SurfCon = Surfactant concentration
TAN = Total acid number
TBN = Total base number
tSI = Shut-in time
UV = Ultraviolet
XRD = X-ray diffraction

REFERENCES

(1) Rassenfoss, S. Permian Leads in Many Ways, Including Rapid Well Declines. *Journal of Petroleum Technology* **2018**, *70*, 39.
(2) Adel, I. A.; Tovar, F. D.; Zhang, F.; Schechter, D. S. The Impact of MMP on Recovery Factor During CO2 – EOR in Unconventional Liquid Reservoirs. In *SPE Annual Technical Conference and Exhibition*; Society of Petroleum Engineers: Dallas, Texas, USA, 2018; p 17.
(3) Alvarez, J. O.; Saputra, I. W. R.; Schechter, D. S. Potential of Improving Oil Recovery with Surfactant Additives to Completion Fluids for the Bakken. *Energy Fuels* **2017**, *31* (6), 5982–5994.
(4) Park, K. H.; Schechter, D. S. Investigation of the Interaction of Surfactant at Variable Salinity with Permian Basin Rock Samples: Completion Enhancement and Application for Enhanced Oil Recovery. In *SPE Liquids-Rich Basins Conference - North America*; Society of Petroleum Engineers: Midland, Texas, USA, 2018; p 20.
(5) Tovar, F. D.; Barrufet, M. A.; Schechter, D. S. Gas Injection for EOR in Organic Rich Shale. Part I: Operational Philosophy. In *SPE Improved Oil Recovery Conference*; Society of Petroleum Engineers: Tulsa, Oklahoma, USA, 2018; p 25.
(6) Tovar, F. D.; Eide, O.; Graue, A.; Schechter, D. S. Experimental Investigation of Enhanced Recovery in Unconventional Liquid Reservoirs using CO2: A Look Ahead to the Future of Unconventional EOR. In *SPE Unconventional Resources Conference*; Society of Petroleum Engineers: The Woodlands, Texas, USA, 2014.
(7) Valluri, M. K.; Alvarez, J. O.; Schechter, D. S. Study of the Rock/Fluid Interactions of Sodium and Calcium Brines with Ultra-Tight Rock Surfaces and their Impact on Improving Oil Recovery by Spontaneous Imbibition. In *SPE Low Perm Symposium*; Society of Petroleum Engineers: Denver, Colorado, USA, 2016.
(8) Zhang, F.; Saputra, I. W. R.; Parsegov, S. G.; Adel, I. A.; Schechter, D. S. Experimental and Numerical Studies of EOR for the Wolfcamp Formation by Surfactant Enriched Completion Fluids and Multi-Cycle Surfactant Injection. In *SPE Hydraulic Fracturing Technology Conference and Exhibition*; Society of Petroleum Engineers: The Woodlands, Texas, USA, 2019; p 24.
(9) Zhang, F.; Adel, I. A.; Park, K. H.; Saputra, I. W. R.; Schechter, D. S. Enhanced Oil Recovery in Unconventional Liquid Reservoir Using a Combination of CO2 Huff-n-Puff and Surfactant-Assisted Spontaneous Imbibition. In *SPE Annual Technical Conference and Exhibition*; Society of Petroleum Engineers: Dallas, Texas, USA, 2018; p 20.
(10) Zhang, F.; Saputra, I. W. R.; Adel, I. A.; Schechter, D. S. Scaling for Wettability Alteration Induced by the Addition of Surfactants in Completion Fluids: Surfactant Selection for Optimum Performance. In *SPE/AAPG/SEG Unconventional Resources Technology Conference*; Unconventional Resources Technology Conference: Houston, Texas, USA, 2018; p 17.
(11) Alvarez, J. O.; Schechter, D. S. Wettability Alteration and Spontaneous Imbibition in Unconventional Liquid Reservoirs by Surfactant Additives. 2017.
(12) Nguyen, D.; Phan, T.; Phan, J.; Hsu, T. P. Investigation of Oil Adhesion to Shale Rocks for EOR. In *SPE International Conference on*

DOI: 10.1021/acs.energyfuels.9b00183
Energy Fuels 2019, 33, 6904–6920

Oilfield Chemistry; Society of Petroleum Engineers: Montgomery, Texas, USA, 2017.
(13) Teklu, T. W.; Li, X.; Zhou, Z.; Alharthy, N.; Wang, L.; Abass, H. Low-salinity water and surfactants for hydraulic fracturing and EOR of shales. *J. Pet. Sci. Eng.* **2018**, *162*, 367−377.
(14) Wang, D.; Zhang, J.; Butler, R.; Koskella, D.; Rabun, R.; Clark, A. Flow Rate Behavior and Imbibition Comparison Between Bakken and Niobrara Formationsrch. In *Unconventional Resources Technology Conference*; Unconventional Resources Technology Conference: Denver, Colorado, USA, 2014.
(15) Alvarez, J. O.; Saputra, I. W. R.; Schechter, D. S. The Impact of Surfactant Imbibition and Adsorption for Improving Oil Recovery in the Wolfcamp and Eagle Ford Reservoirs. In *SPE Annual Technical Conference and Exhibition*; Society of Petroleum Engineers: San Antonio, Texas, USA, 2017; p 25.
(16) Kim, J.; Zhang, H.; Sun, H.; Li, B.; Carman, P. Choosing Surfactants for the Eagle Ford Shale Formation: Guidelines for Maximizing Flowback and Initial Oil Recovery. In *SPE Low Perm Symposium*; Society of Petroleum Engineers: Denver, Colorado, USA, 2016.
(17) Nguyen, D.; Wang, D.; Oladapo, A.; Zhang, J.; Sickorez, J.; Butler, R.; Mueller, B. Evaluation of Surfactants for Oil Recovery Potential in Shale Reservoirs. In *SPE Improved Oil Recovery Symposium*; Society of Petroleum Engineers: Tulsa, Oklahoma, USA, 2014.
(18) Xu, L.; Fu, Q. Ensuring Better Well Stimulation in Unconventional Oil and Gas Formations by Optimizing Surfactant Additives. In *SPE Western Regional Meeting*; Society of Petroleum Engineers: Bakersfield, California, USA, 2012.
(19) Alvarez, J. O.; Schechter, D. S. Wettability, Oil and Rock Characterization of the Most Important Unconventional Liquid Reservoirs in the United States and the Impact on Oil Recovery. In *SPE/AAPG/SEG Unconventional Resources Technology Conference*; Unconventional Resources Technology Conference: San Antonio, Texas, USA, 2016.
(20) Somasundaran, P.; Zhang, L. Adsorption of surfactants on minerals for wettability control in improved oil recovery processes. *J. Pet. Sci. Eng.* **2006**, *52* (1), 198−212.
(21) Kumar, K.; Dao, E. K.; Mohanty, K. K. Atomic Force Microscopy Study of Wettability Alteration by Surfactants. 2008.
(22) Lord, D. L.; Buckley, J. S. An AFM study of the morphological features that affect wetting at crude oil−water−mica interfaces. *Colloids Surf., A* **2002**, *206* (1), 531−546.
(23) Seiedi, O.; Rahbar, M.; Nabipour, M.; Emadi, M. A.; Ghatee, M. H.; Ayatollahi, S. Atomic Force Microscopy (AFM) Investigation on the Surfactant Wettability Alteration Mechanism of Aged Mica Mineral Surfaces. *Energy Fuels* **2011**, *25* (1), 183−188.
(24) Andersen, P. Ø.; Evje, S.; Kleppe, H. A Model for Spontaneous Imbibition as a Mechanism for Oil Recovery in Fractured Reservoirs. *Transp. Porous Media* **2014**, *101* (2), 299−331.
(25) Aronofsky, J. S.; Masse, L.; Natanson, S. G. A Model for the Mechanism of Oil Recovery from the Porous Matrix Due to Water Invasion in Fractured Reservoirs. *Society of Petroleum Engineers* **1958**.
(26) Pooladi-Darvish, M.; Firoozabadi, A. Cocurrent and Countercurrent Imbibition in a Water-Wet Matrix Block. 2000.
(27) Adibhatia, B.; Sun, X.; Mohanty, K. Numerical Studies of Oil Production from Initially Oil-Wet Fracture Blocks by Surfactant Brine Imbibition. In *SPE International Improved Oil Recovery Conference in Asia Pacific*; Society of Petroleum Engineers: Kuala Lumpur, Malaysia, 2005.
(28) Delshad, M.; Najafabadi, N. F.; Anderson, G.; Pope, G. A.; Sepehrnoori, K. Modeling Wettability Alteration By Surfactants in Naturally Fractured Reservoirs. 2009.
(29) Chahardowli, M.; Bruining, H. In *Modeling of Wettability Alteration during Spontanous Imbibition of Mutually Soluble Solvents in Mixed-Wet Fractured Reservoirs*; COMSOL Conference, Cambridge, UK, Cambridge, UK, 2014.
(30) Kalaei, M. H.; Green, D.; Willhite, G. P. A New Dynamic Wettability-Alteration Model for Oil-Wet Cores During Surfactant-Solution Imbibition. 2013.
(31) Kathel, P.; Mohanty, K. K. Wettability Alteration in a Tight Oil Reservoir. *Energy Fuels* **2013**, *27* (11), 6460−6468.
(32) Reed, R. L.; Healy, R. N. Contact Angles for Equilibrated Microemulsion Systems. *SPE-8262-PA* **1984**, *24*, 342.
(33) Saputra, I. W. R.; Schechter, D. S., Comprehensive Workflow for Laboratory to Field-Scale Numerical Simulation to Improve Oil Recovery in the Eagle Ford Shale by Selective Testing and Modelling of Surfactants for Wettability Alteration. In *SPE/AAPG/SEG Unconventional Resources Technology Conference*; Unconventional Resources Technology Conference: Houston, Texas, USA, 2018; p 22.

DOI: 10.1021/acs.energyfuels.9b00183
Energy Fuels 2019, 33, 6904−6920